# ULTRA HIGH IMPEDANCE DIAGNOSTICS OF ELECTROSTATIC ACCELERATORS WITH IMPROVED RESOLUTION

N.R. Lobanov[#], P. Linardakis, D. Tsifakis and T. Tunningley
The Department of Nuclear Physics, Research School of Physics and Engineering,
The Australian National University, Canberra, Australia

## Abstract

This contribution describes a new technique to diagnose faults with high-voltage components in electrostatic accelerators. The main applications of this technique are non-invasive testing of high-voltage grading systems; measuring insulation resistance or determining the volume and surface resistivity of insulation materials used in column posts and acceleration tubes. A simple and practical fault finding data interpretation procedure has been established based on simple concepts. As a result of efficient in-situ troubleshooting and fault elimination techniques, the relative resistance deviation ΔR/R is kept below ±2.5% at the conclusion of maintenance procedures. In 2015 the technique was enhanced by increasing the test voltage from 40 V to 100 V. Experimental verification of the improved resolution was conducted during recent scheduled accelerator maintenance in May-June 2015.

## INTRODUCTION

In electrostatic accelerators, a voltage gradient between electrodes in acceleration tubes is established by resistors conducting current from the high voltage terminal to ground at the entry (low energy) and exit (high energy) of the insulating gas containment tank. The configuration of the 14UD accelerator produced by National Electrostatic Corporation is described in [1]. Typical resistors and ceramic failure modes have been classified by severity in [1–3].

A novel technique to diagnose issues with high-voltage components of electrostatic accelerators is described in [1, 4]. Recently, the resolution of the technique was improved by increasing the test voltage from 40 V to 100 V. The verification of the resolution improvement at higher test voltage is the main purpose of the investigation of this paper. The first section outlines the general concept of high impedance measurement and describes the experimental design, together with the protocols for collecting data and the data analysis procedures. The second section presents key experimental results collected from maintenance performed on the 14UD in May-June 2015 during tank opening (TO) #124. The third section presents the interpretation of the main test results.

## METHODS

A good voltage measuring technique for electrostatic accelerators can be accomplished in the most efficient way by using an electrometer [5]. The basic configuration of the method is shown in Fig. 1.
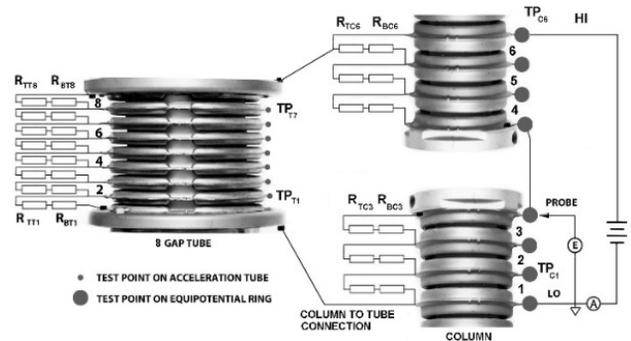
Figure 1: The constant voltage method for diagnostics of the high voltage grading system. The eight gap acceleration tube and the three gaps of the bottom and top section of the column posts are shown. There is a pair of resistors for each column post gap, $R_{TCi}$ and $R_{BCi}$, and a pair for each acceleration tube gap, $R_{TTi}$ and $R_{BTi}$ where $i$ is the gap number. E and A are the electrometers.

The measured voltage distribution across an eight gap acceleration tube and the corresponding six column post gaps is recorded and shown in Table 1. The measurement set up shown in Fig. 1 illustrates the configuration for an eight gap acceleration tube. A voltage of 100 V is applied to six gaps on the column post by connecting cable leads to equipotential rings marked as LO and HI. Through the column to tube connection, this same voltage is consequently applied to the top and bottom gaps of the eight gap tube. The voltages $U_{meas}$ at each test point is recorded. The voltage drop per tube or column gap $U_{gap}$ is then calculated leading to a mean value of voltage drop per gap $<U_{gap}>$. The error value is calculated by $\Delta[\%]=100(U_{gap}/<U_{gap}>-1)$.

For a chain of N identical resistors of value R in series with applied voltage $U_{meas}$, if the value of single resistor is changed by ΔR, the relative resistance change is $\Delta R/R = \Delta U \times N/(U_{meas} - \Delta U)$. The resolution of this method is limited by the electrometer accuracy of the voltage measurement, $\Delta U/U = 0.1\%$. For an eight and eleven gap tube structure and $U_{meas}= 100$ V, the $\Delta R/R_{8GT} = 0.8\%$ and $\Delta R/R_{11GT} = 1.1\%$ correspondingly. For six and five gap post structure and the same test voltage, the calculated $\Delta R/R_{6GP} = 0.6\%$ and $\Delta R/R_{5GP} = 0.5\%$. Evaluation of the data presented in a table provides a feel of what is going on in the high impedance circuit under examination. Components with a measured error above ± 2.5% are considered faulty. In the example results presented in Table 1, two faults are highlighted. It suggests that there

is a lower than expected resistivity in the second tube gap and higher resistance across the second column gap. The comprehensive analysis of a particular pattern collected during the primary non-invasive test is presented in the form of a troubleshooting chart in [1].

Table 1: Voltage Distribution across an Eight Gap Acceleration Tube and the Corresponding Six Gaps on the Column Post with Suspected Faults Highlighted

| $TP_T$ | $U_{meas}$, V | $U_{gap}$, V | $\Delta_T$, % | $TP_C$ | $U_{meas}$, V | $U_{gap}$, V | $\Delta_C$, % |
|---|---|---|---|---|---|---|---|
| 8 | 100.0 | 12.6 | 0.80 | 6 | 100.00 | 16.50 | -1.02 |
| 7 | 87.4 | 12.6 | 0.80 | 5 | 83.50 | 16.40 | -1.62 |
| 6 | 74.8 | 12.5 | 0.00 | 4 | 67.10 | 16.30 | -2.22 |
| 5 | 62.3 | 12.5 | 0.00 | 3 | 50.80 | 16.40 | -1.62 |
| 4 | 49.8 | 12.7 | 1.60 | 2 | 34.40 | 17.60 | 5.58 |
| 3 | 37.1 | 12.5 | 0.00 | 1 | 16.80 | 16.80 | 0.78 |
| 2 | 24.6 | 12.0 | -4.00 | LO | 0.00 | $<U_{gap}>$ | |
| 1 | 12.6 | 12.5 | 0.00 | | | 16.67 | |
| LO | 0.1 | $<U_{gap}>$ | | $TP_T$ - test point on tube | | | |
| | | 12.5 | | $TP_C$ - test point on column | | | |

The adaptors shown in Fig. 2 have been developed to position the sensor on the equipotential rings. The adaptor device shown in Fig. 2 (b) features a shorter slot geometry and more open space between the insulator and the probe tip electrode. This modification substantially reduces electrostatic interference.
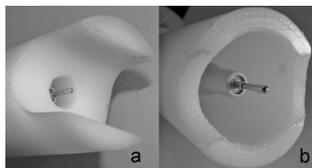


Figure 2: Adaptor devices developed for reproducible positioning of the sensor on equipotential rings.

## RESULTS

The experimental results described in this paper were collected from the 14UD during recent scheduled accelerator maintenance in May-June 2015 (TO#124). The associated Tank Opening Report #124 can be downloaded from http://physics.anu.edu.au/nuclear/tor.php.

Figure 3 and Fig. 4 illustrate the electrometer results of service entry and exit tests of the accelerator resistive grading systems associated with acceleration tubes and column posts. Note that gap voltage distributions do not reflect the actual voltage distribution during accelerator operation, as all distributions are measured at the same test voltage of 100 V, even though there are a different number of gaps. The aim of the exit test is to confirm that the resistive grading system is well balanced within the acceptance margin of ±2.5% after appropriate maintenance has been performed. The chart in Fig. 3 displays the entry and exit distributions of gap voltage in the accelerating tubes. This is also a graphic display of the current configuration of tube resistive dividers taking into account shorted gaps. The entry distribution is shown in red and the exit data presented in green. The horizontal axis is the number of the accelerating tube from low-to high-energy end. Dashed lines display the ±2.5% ac-

ceptance margin at different tube gap voltages $U_{gapT}$, corresponding to the following measurement conditions: 9.1±0.23 V for tubes with eleven gaps; 10.0±0.25 V for eleven gap tubes with one shorted gap; 11.1±0.28 V for eleven gap tubes with two shorted gaps and; 12.5±0.3 V for eight gap tubes.

The chart in Fig. 4 shows the service entry and exit test distributions of gap voltages in the column post structure linked to the acceleration tube by means of column-to-tube connection wires. The horizontal axis is the number of the post gap from the low- to high-energy end of the machine. Dashed lines display ±2.5% acceptance margin at different column gap voltages $U_{gapP}$ corresponding to the following measurement conditions: 16.7±0.4 V for six gaps on posts linked to eight gap tubes; 20.0±0.5 V for five gaps on the posts linked to eleven gap tubes; 22.2±0.56 V for column sections where the voltage distribution is set with nine active resistors and remaining resistors are shorted. In case of sections with five gaps, only one resistor is shorted.
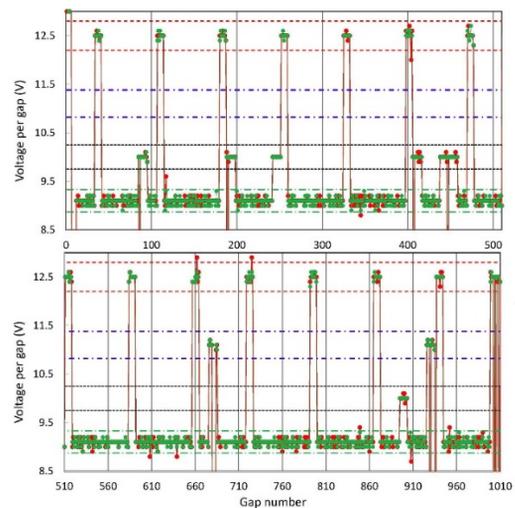


Figure 3: The distribution of gap voltage in the acceleration tubes. The horizontal axis is the gap number in the acceleration tubes starting from low energy to high energy. The red series is the compilation of entry test distribution. The green series is the exit distribution. Dashed lines display the ±2.5% acceptance margin at different gap voltages: dashed/dotted green line is the per gap voltage range 9.1±0.23 V for eleven gap tube; dashed black line is 10.0±0.25 V for eleven gap tube with one shorted gap; dashed/dotted blue line is 11.1±0.28 V for eleven gap tube with two shorted gaps and dashed red line is 12.5±0.3 V for eight gap tube.

A test voltage of 100 V is applied to an assembly incorporating an eleven gap acceleration tube in parallel with five column post gaps or an eight gap acceleration tube in parallel with six gaps on the column post. Each end of an acceleration tube is connected to the column section. In the case of ceramic gap failure in an acceleration tube, a quick fix solution is to short out the gap. Since the number of the gaps on the column post is nearly half of the corresponding number of gaps on the accelera-

tion tube, only one of two resistors bridging across the column post gap is shorted in order to maintain a uniform voltage distribution. The calculated voltage distributions across an arbitrary number of column post gaps is shown in Table 2.
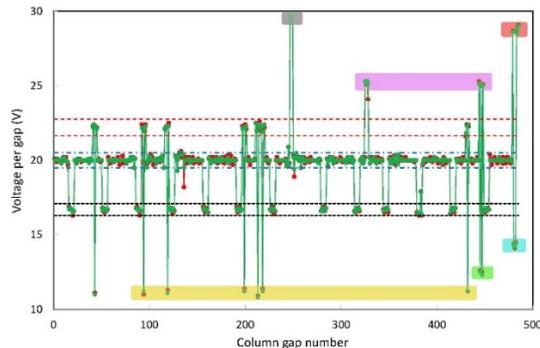


Figure 4: The distribution of gap voltage in the column posts obtained during tests with the electrometer. The horizontal axis is the gap in the column posts numbered from the low-to high-energy end. The red series is the compilation of the entry test distribution accrued during TO#124. The green series is the exit distribution collected in the end of TO#124. Dashed lines display the ±2.5% acceptance margin at different gap voltages: the dashed black line is the per gap voltage margin 16.7±0.4 V for six gaps on the posts linked to eight gap tubes; dashed blue line is 20.0±0.5 V for five gaps on the posts linked to eleven gap tubes; dashed red line is 22.2±0.56 V for five gap posts with one resistor shorted.

Table 2: Calculated Voltage Distribution across an Arbitrary Number of Column Gaps at a Test Voltage of 100 V

| Number of resistors per section | 6 | 7 | 8 | 9 | 10 | 11 | 12 |
|---|---|---|---|---|---|---|---|
| $U_{meas}$ per gap with two resistors | 33.3 | 28.6 | 25.0 | 22.2 | 20.0 | 18.2 | 16.7 |
| $U_{meas}$ per gap with one resistor | 16.7 | 14.3 | 12.5 | 11.1 | 10.0 | 9.1 | 8.3 |

Table 2 represents the current configuration of the resistive divider of the 14UD accelerator. The Data highlighted in Table 2 corresponds to boxes of the same colour shown in Fig. 4. For instance, the column post gaps from the section in which the voltage distribution is set with nine active resistors and remaining resistors shorted can be seen highlighted in yellow in Fig. 4 and Table 2. For this, the voltage per gap containing one resistor is 11.1 V and 22.2 V across gaps with two resistors.

The classification of faults observed during TO#124 is shown in the Pareto chart in Fig. 5.

## DISCUSSION

According to the Pareto chart shown in Fig. 5, the most common failure mode is lack of continuity or poor electrical connection between the column to tube connection at approximately 30%. Of these, failures of the rivet style mountings are the most common.

The next most common fault is an open circuit or poor continuity between pairs of resistors with a fault propor-

tion of 20% for tube resistors and 8% for column post resistors. Pairs of resistors are connected together with a wire inserted into a machined nut at the end of each resistor. The design has proved to be very successful based on operational performance over last two decades. Spark damaged wire leads are still found but are easily replaced.
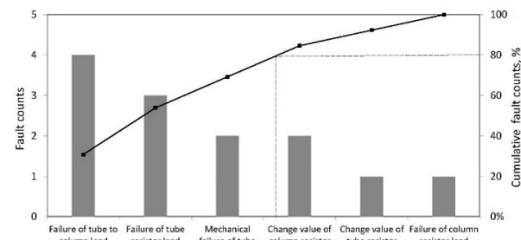


Figure 5: Pareto chart showing the number of 14UD electrostatic structure faults. The dashed line starting at 80% of the right y-axis highlights 80-20 rule.

The next most commonly observed fault category, at 15%, is mechanical failure of the acceleration tube resistor. An example is when the resistor or its spark gap electrode becomes loose in its shield.

The next important fault is a variation of the column post resistor value at 15% or tube resistor value at 8%. The erosion of the resistor conductive layer can occur due to exposure to corona discharge.

The total proportion of faults is 46% for tube components and 23% for column posts. This higher proportion of faults on acceleration tubes is consistent with results reported in [1]. Despite acceleration tubes usually being better protected when compared to column posts, the posts and their resistors are more accessible and historically have been replaced more often as a part of a post refurbishing program.

Finally, the green series in Fig. 3 and Fig. 4 denotes the exit test distribution of gap voltage $U_{gap}$. Overall, it can be seen that as a result of in-situ diagnostics and fault elimination, the maximum deviation of $\Delta U_{gap}$ is kept well within the acceptable level ±2.5%.

## REFERENCES

[1] N.R. Lobanov, P. Linardakis, and D. Tsifakis, Ultrahigh impedance method to assess electrostatic accelerator performance, Phys. Rev. ST Accel. Beams **18**, 060101 (2015).

[2] J. Noe, Proc. Symposium of North Eastern Accelerator Personnel, Notre Dame, France, 1986, pp.168–185.

[3] D.C. Weisser, Nuclear Instruments and Methods in Physics Research Section A, vol. 328, pp. 138–145 (1993).

[4] N.R. Lobanov, P. Linardakis, D. Tsifakis, Nuclear Instruments and Methods in Physics Research Section A, vol. 767, pp. 433–438 (2014).

[5] M.A. Noras, Industry Applications Conference, Industry Applications Conference, 2005. 40th IAS Annual Meeting. Conference Record of the 2005 IEEE, Volume 3, 2–6 Oct., 2005, Hong Kong, pp. 2194–2197.